Effect of Nanoclay Type on Dyeability of Polyethylene Terephthalate/Clay Nanocomposites

Mazeyar Parvinzadeh Gashti,[1] Siamak Moradian[2]

[1]*Department of Textile, Islamic Azad University, Shahre Rey Branch, Tehran, Iran*
[2]*Department of Polymer and Color Engineering, Amirkabir University of Technology, Tehran, Iran*

Received 1 January 2011; accepted 22 March 2011
DOI 10.1002/app.35493
Published online in Wiley Online Library (wileyonlinelibrary.com).

ABSTRACT: Polyethylene terephthalate (PET)-based nanocomposites containing three differently modified clays were prepared by melt compounding. The influence of type of clay on disperseability, thermal, and dyeing properties of the resultant nanocomposite was investigated by various analytic techniques, namely, X-ray diffraction, optical microscopy (OPM), differential scanning calorimetry, thermal gravimetric analysis, dynamical mechanical thermal analysis, contact angle measurement (CAM), reflectance spectroscopy, and light fastness. OPM images illustrated formation of large-sized spherulites in pure PET, while only small-sized crystals appeared in PET/clay nanocomposites. Decreased glass transition temperatures for all PET/clay nanocomposites indicate that the amorphous regions of such composites become mobile at lower temperatures than those in pure PET. CAMs on the resultant PET composites demonstrated that the wettability of such composites depends on hydrophilicity of the nanoclay particles. © 2012 Wiley Periodicals, Inc. J Appl Polym Sci 000: 000–000, 2012

Key words: PET; nanoclay; hydrophilic; hydrophobic

INTRODUCTION

In the recent years, poly(ethylene terephthalate) (PET)-nanometric filler composites have generated significant attention in diverse applications such as transportation vehicles, construction materials, electronics, sporting goods, packaging, household, and textile industries.[1,2] The aim is to enhance a wide range of properties including mechanical properties (modulus, stiffness, and strength), barrier, flame retardancy, solvent and heat resistance, biodegradability, chemical, and thermal stability as well as improvement in dyeability relative to a virgin PET.[3,4] To obtain these specifications, fillers such as cellulose, clay, calcium carbonate, carbon, metal oxides, and various forms of silica have been developed by different researchers. In this regard, the geometrical shape of the particles plays an important role in determining the properties of composites.[5–7]

Processing of such polymeric nanocomposites is more difficult compared to the corresponding pure polymers, because such inorganic nanoparticles have strong tendencies to agglomerate. Several methods are used for preparation of polymeric nanocomposites including sol–gel method, *in situ* polymerization, and melt processing. The last method is still the most cost effective, simple, feasible, and environmentally benign process for the mass production of polymeric nanocomposite.[8–11]

Considerable efforts have been devoted to improve various physical, mechanical, and barrier properties of PET through mixing it with nanoclays.[12–19] The layered clays used are mica, fluoromica, hectorite, saponite, etc., but one of the most commercially interesting clay is bentonite belonging to a structural family known as the 2 : 1 phyllosilicates.[10] It is well known that the clay minerals have also been used as adsorbent for removal of acid, reactive, disperse, and basic dyes from aqueous solutions due to the fact that they are a very abundant and inexpensive materials in the world.[20,21] Their inner layers are composed of an octahedral sheet, which is situated between two tetrahedral sheets. The substitutions of Al^{3+} for Si^{4+} in the tetrahedral layer and Mg^{2+} or Zn^{2+} for Al^{3+} in the octahedral layers result in a net negative surface charge ion in water, which cause the repulsion interaction with anionic dyes.[10]

The dyeability of PET fiber depends on its physical and chemical structure. Dyeing process consists of three steps including the diffusion of dye through the aqueous dyebath on to the fiber, the adsorption of dye into the outer layer of the fiber, and the diffusion of dye from the adsorbed surface into the fiber inside.[22] It was shown by researchers that functional

Correspondence to: M. Parvinzadeh (mparvinzadeh@gmail.com).

groups of PET and water molecules play a great role in this process. The terminal carboxylic and hydroxyl groups in PET chains interact with water molecules. This makes a swelled fiber resulting to increase the attraction of disperse dye by these functional groups of fiber.[23]

The proportion of crystalline and amorphous regions of polymer is another factor influencing the dyeability. The free volume is the only part accessible to disperse dye diffusion above the glass transition temperature of fiber. As PET has relatively hard structure, it is needed to increase the thermal movement of molecular chains with an increase in temperature of dyeing.[24] This polymer has been dyed by a batch system method such as carrier dyeing, high temperature dyeing, and high-pressure steam dyeing to promote diffusion of disperse dyes into the fiber and to obtain a satisfactory dyeing.[22–24] These methods usually consume a lot of energy and water, higher manufacturing costs; a negative effect on some of the bulk properties of the polyester; they may create harsh conditions; they produce undesirable side effects and/or waste disposal problems; there is more waste; the process is highly odorous for workers specially in carrier dyeing; and they require additional energy consumption within the polyester dyeing.[25] Researchers are concerned with the development and implementation of new techniques in order to fulfill improvement in dyeability of polyester. For this purpose, many great studies have been carried out including: physical methods (corona discharge, plasma, ozone-gas, gamma, and microwave functionalizations)[26–36]; chemical methods (enzymatic modification treatment with different reagents, grafting of different monomers, dyeing in supercritical carbon dioxide, and micro-encapsulation techniques),[37–49] and blending of PET with different compounds in fiber production to enhance dyeability.[50–57] However, some of these methods often damage the otherwise excellent mechanical and bulk properties of PET fibers and make stable production thereof difficult. They may result in increased costs of production, which are not offset by the improvements in dyeability. Blending of polymers with nanoclays as inexpensive materials is still claimed as cost-effective method to enhance dyeability.[22–25] Up to now, only two research articles are focused on dyeing properties of polypropylene- and polyamide six-layered clay incorporated nanocomposites prepared by melt compounding.[52,54] Toshniwal et al.[52] suggested that polypropylene fibers could be made dyeable with disperse dyes by addition of nanoclay particles in polymer matrix. Another research work done by Razafimahefa and her colleagues showed that the introduction of the nanoclay improves the dyeing ability of nylon with disperse dyes. Nevertheless, because of the interactions between the anions in montmorillonite and the amino groups on the polyamide, the dyeing sites are occupied with the nanoclay. This leads to a worse dyeing with acid or metal complex dyes than in the case of the unfilled polymer.[54]

PET is the most important man-made fiber with a production of 30.77 million tons in 2009. It is claimed that PET is more preferable than other synthetic polymers from economical and ecological points of view. To avoid decrement of mechanical and thermal properties of PET fibers, nanoclay particles are recommended.[50–57] Dyeability of PET and its compatibility with clay are very important in fiber production and application. All previous research is focused on surface and bulk properties of polyester/clay nanocomposites, and no research has focused on dyeing properties of PET/clay nanocomposites. Such a study is necessary to obtain information on dyeing properties of PET/clay nanocomposites containing one, three, and five percent loads of hydrophilic or hydrophobic nanoclay particles.

EXPERIMENTAL

Materials

Pure PET granules were provided by the Iranian Tondgooyan petrochemical company. Clay particles of montmorillonite type (i.e., Cloisite® 15A, Cloisite® 30B, and Cloisite® Na^+) were supplied by Southern Clay Products (Texas, USA). Their structures are two tetrahedral sheets and one octahedral sheet (2 : 1). The top and bottom are two silica tetrahedral sheets with an aluminum octahedral sheet in the middle. To improve organophilicity, clay may be modified with organic quaternary ammonium compounds. The specifications of nanoclay powders used in this study are shown in Table I. A disperse dye was used for disperse dyeing of PET nanocomposites namely as T/C Brilliant Blue SE-GLT 200% (C. I. Disperse Blue 60 from T & T Industries Corporation (Taiwan; Fig. 1). Acetic acid (85% v/v) from Merck (Germany) was applied for disperse dyeing. The dispersing agent was Ekalin F purchased from Sandoz Company (Switzerland) for the disperse dyeing of PET.

Nanocomposite preparation

PET granules and the three different nanoclay particles were dried in an oven for 24 h at 110°C before the melt processing. Each nanocomposite was prepared by mixing in a C.W. Brabender PL2000 Plasticorder from Germany. The mixing temperature was kept at 255°C in order to ensure proper mix viscosity. The rotation speed was set at 60 rpm for a period of 20 min. The total weight of material per batch was 40 g. The content of each clay particle in the matrix was ensured to be 1, 3, and 5% by weight.

TABLE I
Specifications of the Various Nanoclay Particles Used in This Study

Characteristic properties		Cloisite® 15A	Cloisite® 30B	Cloisite® Na^+
Name of organic modifier		Dimethyl, dehydrogenated tallow, quaternary ammonium	Methyl, tallow, bis-2-hydroxyethyl, quaternary ammonium	None
Chemical constitution of the quaternary ammonium[a]		CH_3 | $CH_3 - N^+ - HT$ | HT	CH_2CH_2OH | $CH_3 - N^+ - T$ | CH_2CH_2OH	–
Modifier concentration		125 meq/100 g clay	90 meq/100 g clay	None
% Moisture		<2	<2	4–9
% Weight loss on ignition		43	30	7
Typical dry particle sizes (μm)	10% less than	2	2	2
	50% less than	6	6	6
	90% less than	13	13	13
Density	Loose bulk (g/cc)	10.79	14.25	12.45
	Packed bulk (g/cc)	18.64	22.71	20.95
	Density (g/cc)	1.66	1.98	2.86
Color		Off white	Off white	Off white
d_{001} (Å)		31.5	18.5	11.7

[a] T is tallow with about 65% C_{18}, 30% C_{16}, and 5% C_{14}. HT is hydrogenated tallow. Anion for the quaternary ammoniums is chloride.

Specimens to be tested were further processed by the aid of a laboratory press under a pressure of 40,000 psi and with a temperature of 260°C for both upper and lower plates. Polyester films of thickness 20 μm were prepared by casting the polymer.

The prepared nanocomposites and pure PET were dyed with the dye at 0.5, 1, and 3% depth of shade. Dyeing was performed using Azar Delta laboratory dyeing machine. Dyeing solutions were prepared by adding the dye, acetic acid (3% v/v), and dispersing agent (3% owf) at a liquor to goods ratio of 30 : 1. Three methods were used for dyeing of composites. Dyeing of all samples was started at 40°C, and the temperature was raised to 100, 110, and 130°C separately for each sample over 20 min and then held at those temperatures for 1 h. The dyed samples were then rinsed in distilled water for 5 min followed by reduction clearing. Reduction clearing was done at 70°C for 10 min in a solution of 6 mL/L, 30% caustic soda, and 4 g/L sodium hydrosulphite at a liquor ratio of 40 : 1. The samples were then rinsed in cold running water followed by neutralizing with acetic acid and rinsed for 5 min in cold running water.

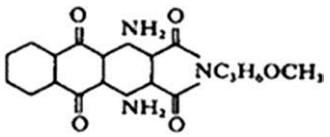

Figure 1 Chemical structure of disperse dye used.

Characterization

Evaluation of morphology

The PET/clay nanocomposite films were characterized with wide-angle X-ray diffractometry using a computerized SEIFERT/PTS 3003 X-ray diffractometer. Ni-filtered Cu Ka radiation generated at 40 kV (k = 0.1542 nm) and 30 mA was used. The measured angle ranged from 1° to 10° and the scan speed of 1°/min.

The optical transparency (or turbidity) of the nanocomposite films was observed with a Projectina 4014 microscope under polarization and crossed polarization. The magnification was at 10× using a CCD camera.

Thermal properties

Calorimetric analysis [differential scanning calorimetry (DSC)] of the pure matrix and the nanocomposites were performed using a Perkin Elmer pyres 6 model integrated with an IBM personal computer. The samples were heated from 30°C up to 300°C at a rate of 5°C/min under nitrogen atmosphere. To gain an insight into the effects of the loaded clay particles on the degree of crystallinity (X_c) of PET matrix, the normalized X_c values of the samples were determined, which can be calculated using the Eq. (1):

$$X_c = (\Delta H_m / \Delta H_m^0) \times 100 \quad (1)$$

where ΔH_m^0 is the melting enthalpy of 100% crystalline PET (ΔH_m^0 = 105.97 J/g[13–16]) and ΔH_m is the normalized melting enthalpy of the sample.

The thermogravimetric analysis (TGA) was performed on a Perkin Elmer thermoanalyzer (Pyris diamond SII). In each case, a 5 mg sample was examined under N_2 at a heating rate of 5°C/min from room temperature to 600°C.

The tensile storage modulus and tensile loss factors of nanocomposite films were measured by a dynamic mechanical thermal analyzer (DMA-TRITON Tritec 2000 DMA model) from Netzsch Company. The scans were made in a single cantilever mode at a constant heating rate of 5°C/min and at a frequency of 1 Hz, from −100 to 200°C.

Surface tension and hydrophilicity

Contact angle measurement and surface-free energy estimation of the nanocomposites were carried out at room temperature on a Kruss G10 instrument of German origin. Surface-free energies of such nanocomposites were estimated by the aid of Owens–Wendt method,[58] using the theory of adhesion work between solid and liquid phases from which polar (γ^P) and nonpolar or dispersive (γ^D) surface-free energies could be derived. Water, diiodo-methane, and benzyl alcohol were used as probe liquids at 23°C ± 2°C and 65% relative humidity. The average contact angle from six different locations on each nanocomposite was determined, and the experimental uncertainty was within ±2°.

Dyeability

Reflectance values of the dyed PET/clay nanocomposites and pure PET were obtained using Gretagmacbeth COLOREYE 7000A spectrophotometer. CIELAB color co-ordinates (L^*, a^*, b^*, C^*, and h) were calculated from the reflectance data for 10° observer and illuminant D_{65}.

Evauation of light fastness properties

The samples were exposed to the daylight for 7 days according to the daylight ISO 105-B01, and the changes in the color (fading) were assessed compared to a blue scale.

RESULTS AND DISCUSSION

Evaluation of morphology by X-ray diffraction

The spacing between clay platelets is used to indicate the extent of intercalation/exfoliation of clay platelets within a polymer composites using X-ray diffraction method. Three different clays were used in this study, and two of them are modified with ammonium salts. Figure 2 gives the XRD patterns of the nanocomposites containing 3% clay minerals in comparison with those of the corresponding clays.

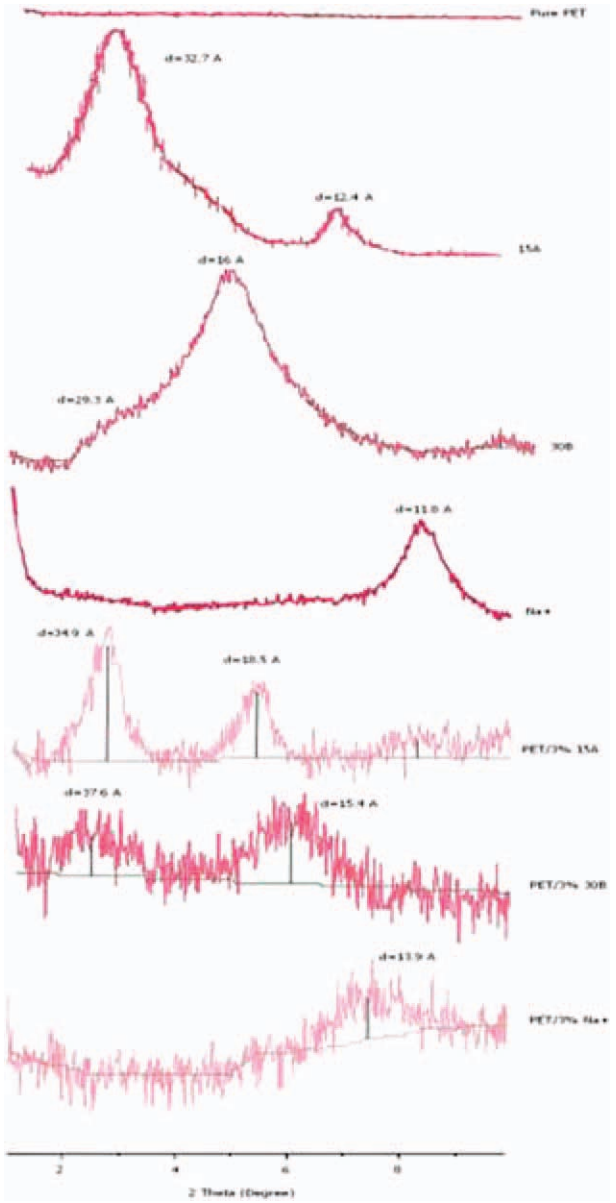

Figure 2 XRD patterns for PET nanocomposites containing 3% clay minerals in comparison with those of the corresponding clays. [Color figure can be viewed in the online issue, which is available at wileyonlinelibrary.com.]

Cloisite® 15A, Cloisite® 30B, and Cloisite® Na^+ have a gallery spacing of 32.7 Å, 29.3 Å, and 11.8 Å, respectively, in the absence of PET. XRD curves indicate a shift in these peaks to 34.9 Å, 37.6 Å, and 13.9 Å for PET/3% 15A, PET/3% 30B, and PET/3% Na^+ nanocomposites, respectively. As the maximum distance between the platelets for Cloisite® 30B was of about 37.6 Å, it can be suggested that its platelets were exfoliated. On the other hand, a slight increase in the gallery spacing for Cloisite® 15A and Cloisite®

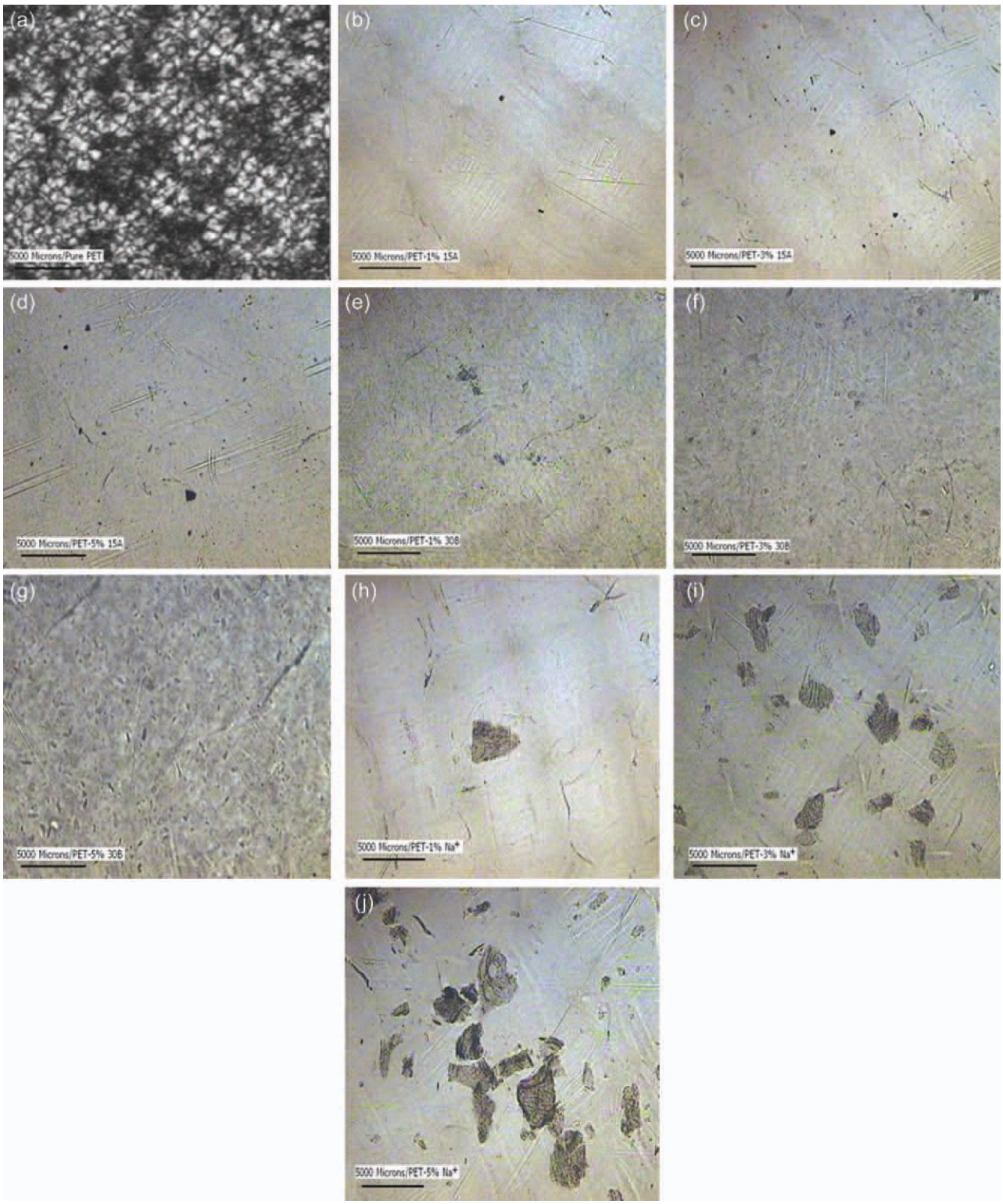

Figure 3 Optical micrographs of various composites (5000 μm): (a) pure PET, (b) PET/1%15A, (c) PET/3%15A, (d) PET/5%15A, (e) PET/1%30B, (f) PET/3%30B, (g) PET/5%30B, (h) PET/1%Na^+, (i) PET/3%Na^+, and (j) PET/5%Na^+. [Color figure can be viewed in the online issue, which is available at wileyonlinelibrary.com.]

TABLE II
Thermal Behavior of Pure PET and Its Various PET/Clay Nanocomposites

Sample	T_g (°C)	T_{onset} (°C)	T_m (°C)	ΔH_m	X_c (%)	T^1_D (°C)	T^5_D (°C)	Wt^{600}_R (%)
Pure PET	93.8	242	254	41.6	39	315.4	393.2	13
PET/5% 15A	89.2	244	255	38.2	36	356.8	381.3	17
PET/5% 30B	89.6	250	256	42.5	40	354.5	385.7	18
PET/5% Na^+	91.0	252	256	38.3	36	382.9	397.8	16

Na^+ suggests that the clay platelets have been intercalated by the PET.

The increased gallery spacing between clay layers observed for the alkyl modified clay nanocomposites is likely because of an increase in compatibility between the modified clays and the PET polymer.[59,60] Other researchers stated that diffusion of polymers through the energetically favorable gallery will maximize contacts with the two confining silicate layers. The adhesive role of PET chains between hydrophilic Cloisite® Na^+ layers strongly prohibit complete dissociation of clay nanoplatelets, usually resulting in only an intercalated state with a limited increase of gallery height.[61–63]

Polarized optical microscopy results

Polarizing optical micrographs of pure PET together with various PET/clay nanocomposites are shown in Figure 3. In pure PET, the crystallites have spherulitic superstructures with distinct maltese patterns. The uniform size of the spherulites indicates uniformly dispersed nucleuses within PET matrix. Most of the spherulites grow up to a diameter of about 2000 μm. Figure 3 shows that the shape of the crystallites in the PET/clay nanocomposites is different from that in pure PET. The spherulites are large in pure PET, while only small-sized crystals appeared in PET clay nanocomposites.

This was probably due to clay nanoparticles dispersed in PET matrix acting as the nucleating agent.[64–66] The optical micrographs also depict the nonuniformity in spherulites after addition of different nanoclay particles. It can be suggested that the strong interaction between PET and modified clays restricted the motions of the PET molecular segment and prohibited the growth of PET crystalline structure. Therefore, smaller and more incomplete crystals formed in PET/15A and PET/30B nanocomposites.

It is well known that surface modification of clay has an important influence on the generation of spherulites in PET nanocomposites. Similar results have been reported elsewhere.[67–70]

Thermal studies

DSC and TGA results of pure PET together with 5% of various nanoclay containing PET composites are given in Table II. DSC is always used to indicate a very high degree of crystal perfection of polymers as well as the presence of molecular chains with different orientation degrees through different peaks. The glass transition temperature is due to molecular movement of PET. There was a decrease in T_g of all PET/clay nanocomposites indicates that the amorphous molecules become mobile at lower temperature than ones in pure PET. The extent of decrease may be due to two different factors. First, the existence of low molecular weight PET chains attached to the clay surface and interlayer may cause a decrease in glass transition temperature of nanocomposites.[71,72] Other factor could be the result of clay agglomeration, which occurs for the addition of clay to the polymer matrix above a critical clay loading. This result was observed by other researchers for PET/5% clay nanocomposites.[73–75] The melting point (T_m) and the onset temperature (T_{onset}) can both reflect the thermal properties of PET nanocomposites. DSC results also showed that T_m and T_{onset} were higher than that of pure PET, 242°C. It can be suggested that the interaction between PET and the nanosized layer of clay was fairly strong. Therefore, it was deduced that the interaction between PET and clay layers worked as crosslinked points of the PET molecular chains. These crosslinked points made the molecular chains more complete and effectively restricted the motions of the molecular segment.[71–74] It is well known that crystallinity affects the polymer and fiber melting point as well as the

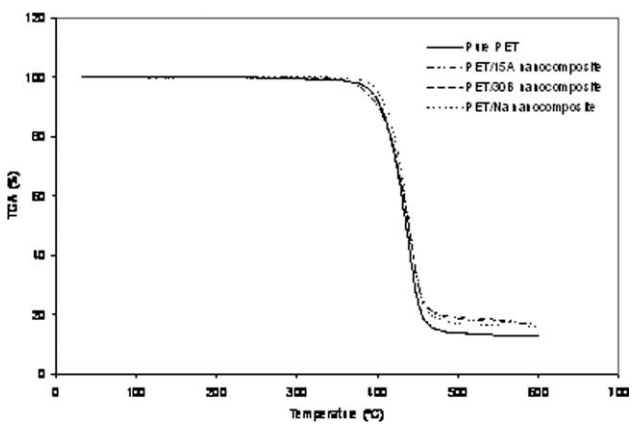

Figure 4 TGA therograms of pure PET and various PET/5% clay nanocomposites.

glass transition temperature.[74] Our DSC results indicated some relationship between crystallinity percentage and glass transition temperature for PET/clay nanocomposites. There was also a decrease in enthalpy and crystallinity percent for PET/clay nanocomposites. The crystallinity of PET is influenced by main-chain flexibility, the nature of any side groups, and crosslinks generated by the presence of nanoclay particles. These results confirm that the clay particles serve as a nucleating agent leading to heterogeneous nucleation at clay loading of 5%. Results for DSC measurements are in agreement with the results obtained from the OPM figures.

Table II and Figure 4 also summarize thermal degradation of PET/5% clay nanocomposites at different temperatures. The weight loss due to decomposition of pure PET and PET/clay nanocomposites was nearly the same until a temperature of about 315°C. After this point, the initial thermal degradation (T^i_D) was influenced by clay loading in PET composite. As can be seen, the T^i_D of PET/clay nanocomposite increased with the addition of nanoclay. The type of nanoclay plays a pivotal role in initial thermal degradation temperature. T^i_D and the temperature at weight reduction of 5% (T^5_D) were observed at 315–383°C and 393–398°C, respectively depending on the nanoclay type used in PET matrix. Results of thermogravimetric analysis show that thermal degradation temperature of PET/Na^+ nanocomposite at different temperatures is more than pure PET, PET/15A, and PET/30B nanocomposites. This can be contributed from two reasons: first, a large amount of hydroxyl groups that exist on the Na^+ clay surface is compatible with terminal carboxylic and hydroxyl functional groups in PET chains, and they are capable to make strong intermolecular interactions.[60–63] Second, organic quaternary ammonium surfactants have been used to modify 15A and 30B clays, which have poor thermal stability at the high temperatures

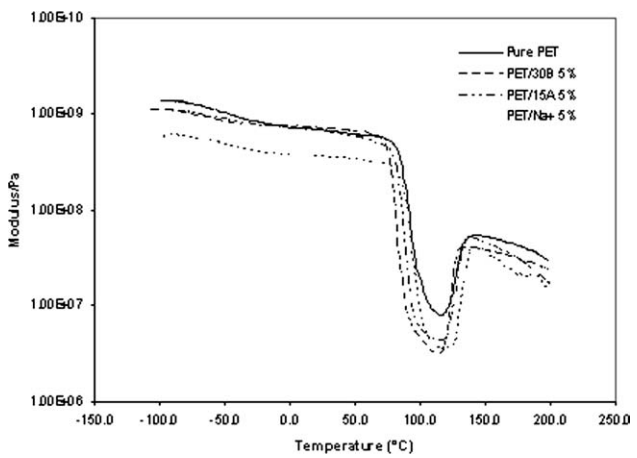

Figure 5 The storage modulus of pure PET and various PET/5% clay nanocomposites.

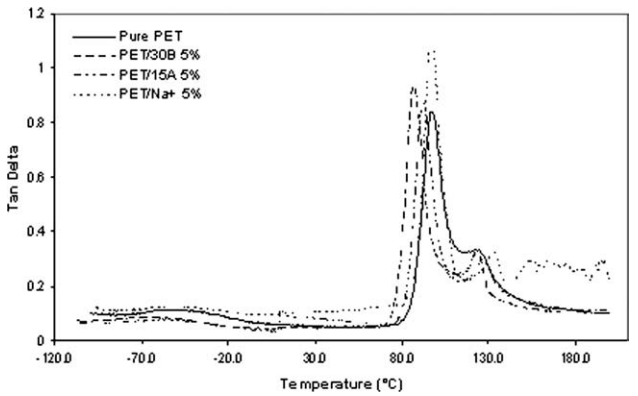

Figure 6 The tan δ of pure PET and PET/5% clay nanocomposites.

during melt processing.[69] As a result, surfactant decomposition also resulted in unwanted side reactions between the decomposition products and the polymer matrix, which could lead to further matrix degradation in PET/15A and PET/30B nanocomposites.[71]

All PET/clay nanocomposites showed weight reduction at relatively higher values compared with pure PET. Weight of the residue at 600°C ($Wt^{600^\circ}_R$) increased for prepared nanocomposites, ranging from 16 to 18%. This enhancement of the char formation is ascribed to the high heat resistance, heat insulation effect, and the mass transport barrier exerted by the nanoclay particles themselves.[62–66] Results showed that the amount of char for PET/15A and PET/30B nanocomposites was the most which is related to the surface modification of nanoclay.

The dynamic mechanical thermal analysis was used to identify interfacial interactions in PET/clay nanocomposites and results are depicted in Figures 5 and 6. The storage modulus of pure PET and various PET/5% clay nanocomposites was distinctively different in the temperature range between −100 and 100°C in Figure 5. It was gradually decreased from −100 to 75°C for pure PET and various PET/clay nanocomposites, which can be associated with the relaxation of amorphous phase. There was a rapid drop below 80°C for all samples due to the glass–rubber transition (T_g). An increase in the cold crystallization range (around 140°C) for pure

TABLE III
Surface Tension of Three Probe Fluids Used in This Study

Probe fluid	Surface tension (mN/m)	γ^D (mN/m)	γ^P (mN/m)
Diiodo-methane	50.8	50.8	0.0
Benzyl alcohol	39.0	28.7	10.3
Water	72.8	21.8	51.0

TABLE IV
Variation in the Surface Free Energy of Nanocomposites as Calculated by Owens Method

Sample	Average contact angle (°)			γ^D (mJ/m^2)	γ^P (mJ/m^2)	γ^T (mJ/m^2)
	Diiodo-methane	Benzyl alcohol	Water			
Pure PET	67.4	56.7	96.7	24.12	1.64	25.76
PET/5% 15A	60.6	47.6	95.3	28.60	1.31	29.92
PET/5% 30B	57.5	45.6	95.8	30.51	0.98	31.49
PET/5% Na^+	54.0	43.3	95.9	32.5	0.75	33.25

PET and various PET/clay nanocomposites is related to composite reinforcing by the crystallites being formed. A decrease in modulus values for nanocomposites at higher temperatures of 140°C is relevant to premelting process. As can be seen, modulus values for various PET/clay nanocomposites at temperatures around T_g were lower than pure PET, which confirms the results obtained from DSC measurements.

The dependencies of tan δ on temperature for PET nanocomposites are shown in Figure 6. The maximum in tan δ about 80–90°C corresponds to segmental relaxation related to the glass–rubber transition in PET nanocomposites. The tan δ value at peaks related to the T_g region are higher for PET/Na^+ compared to other nanocomposites. This is attributed to the nature of Na^+ clay and its surface properties that contains a large amount of OH groups and affects the interactions of PET-Na^+ matrix and lower segmental motions of PET chains resulting to increase the tan δ value. This result was confirmed by other authors in Na^+-filled PET composite.[69–72] Another peak appeared at higher temperatures around 120–140°C reflects an increase of the mechanical loss due to the cold crystallization. Its intensity and temperature varied for different nanoclay particles used.[75]

Contact Angle and Free Energy Analysis

Three probe fluids of diiodo-methane, benzyl alcohol, and water were used in this study, and their surface tensions, polar (γ^P), and nonpolar or

TABLE V
Color Coordinates of Pure PET and Its Various PET/Clay Nanocomposites Dyed with a Disperse Dye at 100°C

Composite type	Clay (%)	Dye (%)	L^*	a^*	b^*	C^*	$h°$
Pure PET	0	0.5	64.06	−13.73	−6.75	15.30	206.17
PET/15A	1	0.5	63.35	−13.73	−6.89	15.83	209.89
	3	0.5	52.71	−13.79	−5.64	15.74	203.27
	5	0.5	50.71	−14.53	−4.65	15.59	201.27
PET/30B	1	0.5	59.22	−13.74	−6.85	15.05	209.35
	3	0.5	50.64	−13.89	−1.76	9.06	191.22
	5	0.5	50.24	−13.23	−0.97	8.29	186.72
PET/Na^+	1	0.5	64.09	−13.78	−6.78	15.69	216.73
	3	0.5	64.50	−14.04	−6.67	16.22	203.52
	5	0.5	67.18	−15.20	−9.30	19.97	213.21
Pure PET	0	1	59.81	−14.34	−11.73	18.53	291.28
PET/15A	1	1	57.55	−15.38	−10.79	18.79	215.04
	3	1	52.16	−15.67	−6.01	17.34	198.98
	5	1	51.06	−16.06	−4.49	12.32	202.00
PET/30B	1	1	54.64	−14.32	−11.44	18.76	213.45
	3	1	49.09	−14.84	−4.11	12.66	202.69
	5	1	47.51	−14.17	−4.52	10.98	200.39
PET/Na^+	1	1	59.49	−15.75	−11.66	18.60	216.52
	3	1	63.08	−15.95	−11.59	18.66	205.46
	5	1	63.18	−15.91	−11.96	19.77	212.04
Pure PET	0	3	62.37	−16.31	−9.98	19.12	211.46
PET/15A	1	3	57.06	−16.35	−9.29	19.48	219.47
	3	3	50.78	−16.09	−9.67	18.11	235.82
	5	3	45.82	−16.08	−6.84	17.47	203.05
PET/30B	1	3	54.50	−16.27	−8.89	18.54	208.65
	3	3	52.86	−16.28	−3.83	12.92	198.73
	5	3	47.28	−16.84	−2.93	11.20	193.92
PET/Na^+	1	3	62.68	−16.82	−11.38	20.29	216.89
	3	3	64.32	−16.00	−12.56	21.25	191.13
	5	3	65.00	−17.71	−13.56	22.32	214.66

TABLE VI
Color Coordinates of Pure PET and Its Various PET/Clay Nanocomposites Dyed with a Disperse Dye at 110°C

Composite type	Clay (%)	Dye (%)	L^*	a^*	b^*	C^*	h°
Pure PET	0	0.5	51.15	−19.48	−31.24	36.82	238.05
PET/15A	1	0.5	51.53	−19.21	−23.24	30.80	228.99
	3	0.5	51.30	−19.42	−18.93	28.90	215.86
	5	0.5	49.47	−19.89	−16.38	27.09	222.73
PET/30B	1	0.5	51.37	−19.78	−21.65	28.66	229.06
	3	0.5	46.64	−18.30	−14.91	25.03	216.56
	5	0.5	45.11	−18.20	−14.33	24.12	216.46
PET/Na^+	1	0.5	57.67	−19.66	−31.47	36.45	229.00
	3	0.5	58.62	−20.47	−33.87	37.62	230.31
	5	0.5	69.82	−21.70	−33.84	37.10	226.53
Pure PET	0	1	49.33	−21.57	−32.16	38.73	236.15
PET/15A	1	1	49.09	−21.00	−31.25	33.84	247.41
	3	1	49.42	−22.87	−23.32	32.66	225.55
	5	1	48.10	−27.95	−13.69	23.25	225.50
PET/30B	1	1	44.26	−21.10	−25.43	33.69	229.00
	3	1	39.48	−21.28	−14.41	21.75	221.50
	5	1	39.20	−21.06	−13.50	20.22	221.87
PET/Na^+	1	1	56.10	−21.88	−32.39	38.45	234.23
	3	1	57.26	−21.69	−33.31	38.51	230.27
	5	1	59.09	−21.18	−33.57	38.39	230.87
Pure PET	0	3	55.40	−22.65	−23.69	32.77	226.28
PET/15A	1	3	52.39	−22.31	−23.98	31.01	230.41
	3	3	50.81	−22.55	−22.11	27.03	234.86
	5	3	47.82	−22.02	−16.81	26.92	218.64
PET/30B	1	3	49.62	−22.61	−21.01	30.42	230.02
	3	3	45.65	−22.13	−17.21	28.67	219.98
	5	3	45.98	−22.65	−15.59	27.89	219.10
PET/Na^+	1	3	55.39	−22.81	−23.28	32.88	247.06
	3	3	55.82	−22.55	−25.52	32.81	229.62
	5	3	56.94	−22.58	−26.53	33.43	229.79

dispersive (γ^D) surface-free energies are given in Table III. Table IV also shows variation in surface-free energy of nanocomposites as calculated by the Owens method. All nanoclays embedded in the PET matrix decreased the average contact angles for all liquids used while average contact angles of water for all PET/clay nanocomposites was very close to pure PET. The nanoclays also increased dispersive surface-free energy and decreased polar surface-free energy for PET composites resulting in a net increase in the total surface-free energy. Variations in γ^T for PET nanocomposites depend on the relative hydrophilicity of clays used. Nanoclay of 15A has methyl groups on its surface, and so it is more hydrophobic while 30B nanoclay has more polar groups, which makes it more hydrophilic compared to 15A clay. The surface properties of 15A clay make it more compatible with PET molecular chains resulting in only small increases in total surface-free energy and surface roughness.[10,11]

It is well known that clay particles usually have very large aspect ratio. The adsorption and desorption of water from clay layers depend on the concentration and type of surface polar groups, specific surface area, average particle size, and type of packing of primary particles in aggregates. Obviously, as chemical end groups of PET chains are limited, therefore particles with higher surface free energy do not distribute evenly into the PET composite. In contrast, surface-treated clay nanoparticles attempt to reside in the polymer bulk, and they are more compatible with the PET matrix.[10,11,15,20]

Dyeing properties

The L^*, a^*, b^*, C^*, and h° values of pure PET and its various nanoclay composites dyed with a disperse dye at 100, 110, and 130°C are given in Tables V–VII. The color values were evaluated in CIELAB color space, the three axes namely as L^*, a^*, and b^*. The L^* is the color coordinate that represents the lightness of samples and can be measured independently of color hue. Any decrease in the lightness of samples could be concluded as the more color absorption into the composite. The a^* stands for the horizontal red-green color axis. The b^* represents the vertical yellow-blue axis. The C^* represents brightness or dullness of the samples. Any increase in the C^* of samples could be concluded as more brightness of the composite.[76]

According to the results, the lightness (L^*) and brightness (C^*) values decreased for the PET/1% 15A and PET/1% 30B nanocomposites after dyeing

TABLE VII
Color Coordinates of Pure PET and Its Various PET/Clay Nanocomposites Dyed with a Disperse Dye at 130°C

Composite type	Clay (%)	Dye (%)	L^*	a^*	b^*	C^*	h°
Pure PET	0	0.5	49.01	−20.73	−19.11	28.20	222.66
PET/15A	1	0.5	49.66	−19.37	−16.63	28.37	221.99
	3	0.5	49.11	−20.84	−15.76	26.56	219.90
	5	0.5	43.92	−20.24	−14.80	24.30	219.69
PET/30B	1	0.5	49.37	−20.71	−19.94	25.54	217.79
	3	0.5	47.42	−20.85	−19.54	24.01	225.98
	5	0.5	47.41	−21.55	−11.76	24.55	208.62
PET/Na^+	1	0.5	54.90	−20.81	−20.97	28.67	234.31
	3	0.5	54.22	−20.04	−25.80	32.67	232.15
	5	0.5	56.41	−20.08	−28.33	35.58	225.36
Pure PET	0	1	45.14	−10.84	−30.44	32.31	250.39
PET/15A	1	1	45.10	−11.93	−28.72	32.75	231.39
	3	1	45.61	−11.54	−27.52	31.13	242.14
	5	1	44.39	−10.75	−15.53	24.35	219.62
PET/30B	1	1	42.02	−11.68	−30.18	28.90	243.29
	3	1	41.36	−11.86	−20.39	25.43	232.54
	5	1	41.68	−11.88	−19.40	24.25	233.88
PET/Na^+	1	1	50.52	−19.18	−30.44	32.18	242.24
	3	1	54.25	−22.41	−36.09	32.48	238.16
	5	1	59.20	−22.83	−36.23	36.13	254.85
Pure PET	0	3	37.72	−0.08	−35.04	35.04	269.85
PET/15A	1	3	34.39	−0.09	−32.87	33.13	262.89
	3	3	34.45	−0.63	−26.90	27.95	266.53
	5	3	32.06	−0.67	−22.41	26.35	235.03
PET/30B	1	3	33.80	−0.84	−30.84	30.90	266.07
	3	3	32.50	−0.61	−26.60	26.81	263.26
	5	3	32.01	−0.70	−25.62	25.88	261.67
PET/Na^+	1	3	38.95	−0.40	−35.90	35.98	266.46
	3	3	43.31	−0.93	−36.55	35.56	268.39
	5	3	43.50	−0.61	−38.02	38.03	268.96

at different temperatures followed by more decrease as the nanoclays concentration increased in nanocomposite. Decrease in L^* values could be due to more disperse dye penetration into the composite samples. In other words, any decrease in C^* resulting to increase in dullness of composites. The differences between a^* values for composites containing modified clays compared to pure PET were negligible. The a^* and b^* values of disperse dyed samples were influenced by type of clay used in matrix. There were some considerable increases in L^*, a^*, b^*, and C^* values for PET/Na^+ nanocomposites dyed with disperse dye at different temperatures, which were in contrast to those of PET/15A and PET/30B nanocomposite samples.

From colorimetric tables, it is evident that a positive correlation exists between the type of clay, its content, and the dye absorbed by the nanocomposites. As mentioned earlier, disperse dyeing behavior of PET composite depends on the affinity of the dye to the polymer, chemical structure of disperse dye, existence of active area, and crystallinity percent in the polymer.[77,78] The amount of active area was increased with an increase in temperature as well as incorporation of modified clays in polyester. In this regard, the hydrophobic character of polyester plays a dominant role in disperse dyeing. Both 15A and 30B clays have a strong sorption ability to disperse dyes despite their hydrophobicity and lack of aromatic rings.[79] Their small size and huge surface area are necessary for a good sorbent.

Nanoclay of Na^+ is natural montmorillonite carries a negative charge, while 15A and 30B clays are modified with surfactants to provide a positive charge on clay surface. It seems that active centers of disperse dye molecule including NH_2 and CO groups can participate in either type of bond formation. Our previous study demonstrated that nanoclays contain surface hydroxyl groups, which seem to increase the interfacial interactions and bonding with the carboxyl or hydroxyl end groups of PET chains. These interactions are observed between clays and PET chains. PET chains are more compatible with hydrophobic nanoclay particles of 15A and 30B compared to the hydrophilic Na^+.[57] The following type of interactions between the anthraquinone disperse dye and modified clay surfaces are possible:

- Hydrogen bonding between OH groups of 30B clay and the NH_2 and CO groups of disperse dye molecule.
- Electrostatic bonding between the negatively charged oxygen atom of carbonyl groups in

TABLE VIII
Light Fastness of Pure PET and Its Various PET/Clay Nanocomposites Dyed with a Disperse Dye at Different Temperatures

		Dyeing temperature (°C)								
		100°C			110°C			130°C		
Composite type	Clay (%)	0.5%	1%	3%	0.5%	1%	3%	0.5%	1%	3%
Pure PET	0	5	5	5	5	5	6	5	5	6
PET/15A	1	5	5	5	5	5	6	5	5	6
	3	5	5	5	5	5	6	5	5	6
	5	5	5	5	5	5	6	5	5	6
PET/30B	1	5	5	5	5	5	6	5	5	6
	3	5	5	5	5	5	6	5	5	6
	5	5	5	5	5	5	6	5	5	6
PET/Na^+	1	5	5	5	5	5	6	5	5	6
	3	5	5	5	5	5	6	5	5	6
	5	5	5	5	5	5	6	5	5	6

disperse dye molecule and positively charged nitrogen atom of quaternary ammonium salt in modified clays.
- Direct π interactions and van der Waals forces between methyl and ethyl groups of modified clays on one hand and methoxy group and benzene rings of disperse dye molecule on the other hand.

Another reason for improving disperse dye absorption of PET/15A and PET/30B nanocomposites could be the relatively large voids between clay platelets after modification with quaternary ammonium salts. Our results in dyeability of polyester are confirmed by other authors in polypropylene/clay nanocomposite.[52] The accessibility of polyester would be enhanced by the incorporation of reactive silica nanoparticles and modified clays. Some researchers stated that the presence of clay nanoparticles in polypropylene and nylon 6 matrixes resulted in the increase of void spaces and tortuous pathways generated by oriented nanoclay layers. These spaces are necessary for modifying the fiber structure, and it is useful for penetration of the disperse dye from the surface into the interior of the polymer.

Light fastness measurement

Light fastness rating of pure PET and its clay nanocomposite films is shown in Table VIII. For this purpose, eight pieces of different dyed fabrics that form the blue scale were exposed to the light at the same time as the test was preceded for the nanocomposite specimens in order to determine any differences between samples. After exposure, the degree of fading of the test specimen was compared to the blue scale. In this test, any result above five of eight is considered as the good light fastness.[79]

After exposure to light, no noticeable fading of nanocomposites was observed. Many factors influence the light fastness of dyes, including the chemical state of the dye, the physical state of the dye within the fibers and polymers, the polymer substrate, dye concentration in the fibers, dye environmental factors, the source and intensity of illumination, and the presence of UV absorbers and application of other finishing materials after dyeing.[80–91] Previous researches indicated that disperse dyed clay incorporated PP nanocomposite fibers exhibit satisfactory light fastness, which is due to intermolecular interaction between dye, modified clay and substrate.[52]

CONCLUSION

Various PET/clay nanocomposites were prepared by melt spinning. The experiments carried out in DSC showed that the presence of clay in PET affects the crystallization of polymer, decreasing the glass transition temperature and leading to heterogeneous nucleation of composite. The accessibility of PET filled with modified clays is thus improved due to hydrogen and electrostatic bondings as well as van der Waals interactions between the disperse dye used and modified clay surfaces. We suggest modified clays of 30B and 15A to be used in PET composites to improve dyeability.

References

1. Ray, S. S.; Okamoto, M. Prog Polym Sci 2003, 28, 1539.
2. Leszczyńska, A.; Njuguna, J.; Pielichowski, K.; Banerjee, J. R. Thermochim Acta 2007, 453, 75.
3. Leszczyńska, A.; Njuguna, J.; Pielichowski, K.; Banerjee, J. R. Thermochim Acta 2007, 454, 1.
4. Pesetskii, S. S.; Bogdanovich, S. P.; Myshkin, N. K. J Fric Wear 2007, 28, 457.
5. Bhat, G.; Hegde, R. R.; Kamath, M. G.; Deshpande, B. J. Eng Fiber Fabric 2008, 3, 22.
6. Njuguna, J.; Pielichowski, K.; Desai, S. Polym Adv Technol 2008, 19, 947.
7. Ma, J.; Xu, J.; Ren, J. H.; Yu, Z. Z.; Mai, Y. W. Polymer 2003, 44, 4619.
8. Burgentzlé, D.; Duchet, J.; Gérard, J. F.; Jupin, A.; Fillon, B. J Colloid Interf Sci 2004, 278, 26.

9. Modestia, M.; Bescoa, S.; Lorenzettia, A.; Causinb, V.; Maregab, C.; Gilmanc, J. W.; Foxd, D. M.; Trulovee, P. C.; De Longf, H. C.; Zammarano, M. Polym Degrad Stab 2007, 92, 2206.
10. Xanthos, M. Functional Fillers for Plastics; Wiley: Weinheim, 2005; p 163–174.
11. Paiva, L. B. D.; Morales, A. R.; Dı'az, F. R. V. Appl Clay Sci 2008, 42, 8.
12. Chung, J. W.; Son, S. B.; Chun, S. W.; Kang, T. J.; Kwak, S. Y. Polym Degrad Stab 2008, 93, 252.
13. Costache, M. C.; Heidecker, M. J.; Manias, E.; Wilkie, C. A. Polym Adv Technol 2006, 17, 764.
14. Choi, W. J.; Kin, H. J.; Yoon, K. H.; Kwon, O. H.; Hwang, C. I. J Appl Polym Sci 2006, 100, 4875.
15. Calcagno, C. I. W.; Mariani, C. M.; Teixeira, S. R.; Mauler, R. S. Polymer 2007, 48, 966.
16. Jawahar, P.; Gnanamoorthy, R.; Balasubramanian, M. J Mater Sci 2005, 40, 4391.
17. Ou, C. F.; Ho, M. T.; Lin, J. R. J Appl Polym Sci 2004, 91, 140.
18. Wan, T.; Chen, L.; Chua, Y. C.; Lu, X. J Appl Polym Sci 2004, 94, 1381.
19. Phang, Y.; Pramoda, K. P.; Liu, T.; He, C. Polym Int 2004, 53, 1282.
20. Ozacar, M.; Sengil, I. A. Environ Geol 2004, 45, 762.
21. Ozcan, S.; Erdem, B.; Ozcan, A. Colloid Surf B 2005, 266, 73.
22. Lewin, M. Handbook of Fiber Chemistry; CRC Press: FL, 2007; p 150.
23. Kirk-Othmer. Encyclopedia of Chemical Technology, Vol.8; Wiley-VCH: New York, 1998; p 784.
24. Fourne, F. Synthetic Fibers; Hanser: Munich, 1999; p 139.
25. McIntyre, J. E. Synthetic Fibers: Nylon, Polyester, Acrylic, Polyolefin. Woodhead: Cambridge, 2005; p 25.
26. Xu, W.; Liu, X. Eur Polym J 2003, 39, 199.
27. Morent, R.; Geyter, N. D.; Leys, C.; Gengembre, L.; Payen, E. Text Res J 2007, 77, 471.
28. Xu, W.; Yang, C. Color Technol 2002, 118, 211.
29. Zohdy, M. H. Radiat Phys Chem 2005, 73, 101.
30. Lee, M.; Lee, M. S.; Wakida, T.; Tokuyama, T.; Inoue, G.; Ishida, S.; Itazu, T.; Miyaji, Y. J Appl Polym Sci 2006, 100, 1344.
31. Gupta, D.; Siddhan, P.; Banerjee, A. Color Technol 2007, 123, 248.
32. Acar, M.; Dudeney, W. L.; Jones, J.; Jackson, M. R.; Malalasekera, W. J Indust Text 2005, 34, 181.
33. Knittel, D.; Schollmeyer, E. Polym Int 1998, 45, 110.
34. Yip, J.; Chan, K.; Sina, K. M.; Lau, K. S. Color Technol 2002, 118, 31.
35. Kan, C. W. Opt Laser Technol 2008, 40, 113.
36. Shaohua, L.; Xiang, Z.; Tianmin, T.; Zhiqi, X.; Qihong, L. Color Technol 2003, 119, 19.
37. Guebitz, G. M.; Cavaco-Paulo, A. Trend Biotech 2008, 26, 32.
38. Parvinzadeh, M. Color Technol 2009, 125, 228.
39. Parvinzadeh, M.; Assefipour, R.; Kiumarsi, A. Polym Degrad Stab 2009, 94, 1197.
40. Kiumarsi, A.; Parvinzadeh, M. J Appl Polym Sci 2010, 116, 3140.
41. Bendak, A.; Raslan, W. M. J Appl Polym Sci 2007, 108, 7.
42. Rajendran, S.; Ramasamy, S. S.; Mishra, S. P. J Appl Polym Sci 1998, 62, 989.
43. Celik, M.; Sackak, M. J Appl Polym Sci 1996, 59, 609.
44. Coskun, R.; Sacak, M.; Karaksla, M. J Appl Polym Sci 2005, 97, 1795.
45. Arslan, M.; Yigitoglu, M. J Appl Polym Sci 2007, 107, 2846.
46. Faterpekar, S. A.; Potnis, S. P. Text Res J 1981, 51, 448.
47. Hou, A.; Xie, K.; Dai, J. J Appl Polym Sci 2004, 92, 2008.
48. Kraan, M. V. D.; Cid, M. V. F.; Woerlee, G. F.; Veugelers, W. J. T.; Witkamp, G. J. J Supercrit Fluid 2007, 40, 470.
49. Leelajariyakul, S.; Noguchi, H.; Kiatkamjornwong, S. Prog Org Coat 2008, 62, 145.
50. Yue, Q. Y.; Lia, Q.; Gao, B. Y.; Yuan, A. J.; Wang, Y. Appl Clay Sci 2007, 35, 268.
51. Yang, Y.; Han, S.; Fan, Q.; Ugbolue, S. C. Text Res J 2005, 75, 622.
52. Toshniwal, L.; Fan, Q.; Ugbolue, S. C. J Appl Polym Sci 2007, 106, 706.
53. Froehling, P. E. Dyes Pigments 2001, 48, 187.
54. Razafimahefa, L.; Chlebicki, S.; Vroman, I.; Devaux, E. Dyes Pigments 2005, 66, 55.
55. Yang, Y.; Gu, H. J Appl Polym Sci 2007, 105, 2363.
56. Parvinzadeh, M.; Moradian, S.; Rashidi, A.; Yazdanshenas, M. E. Appl Surf Sci 2010, 256, 2792.
57. Parvinzadeh, M.; Moradian, S.; Rashidi, A.; Yazdanshenas, M. E. Polym-Plast Technol 2010, 49, 874.
58. Geoghegan, M.; Krausch, G. Prog Polym Sci 2003, 28, 261.
59. Xu, X.; Ding, Y.; Qian, Z.; Wang, F.; Wen, B.; Zhou, H.; Zhang, S.; Yang, M. Polym Degrad Stab 2009, 94, 113.
60. Davis, C. H.; Mathias, L. J.; Gilman, J. W.; Schiraldi, D. A.; Shields, J. R.; Trulove, P.; Sutto, T. E.; Delong, H. C. J Polym Sci Polym Phys 2002, 40, 2661.
61. Al-Khanbashi, A.; El-Gamal, M.; Moet, A. J Appl Polym Sci 2005, 98, 767.
62. Guan, G.; Li, C.; Yuan, X.; Xiao, Y.; Liu, X.; Zhang, D. J Polym Sci Polym Phys 2008, 46, 2380.
63. Hwang, S. Y.; Lee, W. D.; Lim, J. S.; Park, K. H.; Im, S. S. J Polym Sci Polym Phys 2008, 46, 1022.
64. Kim, S. H.; Park, S. H.; Kim, S. C. Polym Bull 2005, 53, 285.
65. Pollet, E.; Delcourt, C.; Alexandre, M.; Dubois, P. Eur Polym J 2006, 42, 1330.
66. Wang, Y.; Shen, C.; Li, H.; Li, Q.; Chen, J. J Appl Polym Sci 2004, 91, 308.
67. Chang, J. H.; Kim, S. J.; Joo, Y. L.; Im, S. Polymer 2004, 45, 919.
68. Chang, J. H.; Mun, M. K.; Lee, I. C. J Appl Polym Sci 2005, 98, 2009.
69. Guan, G. H.; Li, C. C.; Zhang, D. J Appl Polym Sci 2005, 95, 1443.
70. Xiao, W.; Yu, H.; Han, K.; Yu, M. J Appl Polym Sci 2005, 96, 2247.
71. Chang, J. H.; Mun, M. K. Polym Int 2007, 56, 57.
72. Gianelli, W.; Camino, G.; Tabuani, D.; Bortolon, V.; Savadori, T.; Monticelli, O., Fire Mater 2006, 30, 333.
73. Barber, G. D.; Calhoun, B. H.; Moore, R. B. Polymer 2005, 46, 6706.
74. Ammala, A.; Bell, C.; Dean, K. Compos Sci Technol 2008, 68, 1328.
75. Laia, M. C.; Chang, K. C.; Huang, W. C.; Hsua, S. C.; Yeha, J. M. J Phys Chem Solids 2008, 69, 1371.
76. Balazsy, A. T.; Eastop, D. Chemical Principles of Textile Conservation; Wiley: New York, 1998; p 36.
77. Gulrajani, M.; Gupta, D. B.; Agarwal, V.; Jain, M. Indian Text J 1992, 102, 50.
78. Trotman, E. R. Dyeing and Chemical Technology of Textile Fibers, 5th ed.; Hodder & Stoughton: London, 1975; p 321.
79. Yue, Q. Y.; Li, Q.; Gao, B. Y.; Yuan, A. J.; Wang, Y. Appl Clay Sci 2007, 35, 268.
80. Oakes, J. Rev Prog Color 2001, 31, 21.
81. Wendelin, M. R.; Crews, P. C. Text Res J 1993, 4, 231.
82. Montazer, M.; Parvinzadeh, M. J Appl Polym Sci 2004, 93, 2704.
83. Parvinzadeh, M. J Surfact Deterg 2007, 10, 219.
84. Parvinzadeh, M.; Najafi, H. Tenside Surfact Deterg 2008, 45, 13.
85. Parvinzadeh, M.; Ebrahimi, I. Appl Surf Sci 2011, 257, 4062.
86. Parvinzadeh, M.; Ebrahimi, I. Radiat Eff Def Solids 2011, 166, 408.
87. Hajiraissi, R.; Parvinzadeh, M. Appl Surf Sci 2011, 257, 8443.
88. Rahimi, M. H.; Parvinzadeh, M.; Yousefpour Navid, M.; Ahmadi, S. J Surfact Deterg 2011, 14, 595.
89. Parvinzadeh, M. Res J Chem Environ 2009, 13, 49.
90. Parvinzadeh, M.; Eslami, S. Res Chem Interm 2011, 37, 771.
91. Parvinzadeh, M. Enzym Microb Technol 2007, 40, 1719.